
logLTN: Differentiable Fuzzy Logic in the Logarithm Space

Samy Badreddine

Sony AI
Tokyo
Japan
samy.badreddine@sony.com

Luciano Serafini

Fondazione Bruno Kessler
Trento
Italy
serafini@fbk.eu

Michael Spranger

Sony AI
Tokyo
Japan
michael.spranger@sony.com

Abstract

The AI community is increasingly focused on merging logic with deep learning to create Neuro-Symbolic (NeSy) paradigms and assist neural approaches with symbolic knowledge. A significant trend in the literature involves integrating axioms and facts in loss functions by grounding logical symbols with neural networks and operators with fuzzy semantics. Logic Tensor Networks (LTN) is one of the leading representatives in this category, known for its simplicity, efficiency, and versatility. However, it has been previously shown that not all fuzzy operators perform equally when applied in a differentiable setting. Researchers have proposed several configurations of operators, trading off between effectiveness, numerical stability, and generalization to different formulas. This paper presents a configuration of fuzzy operators for grounding formulas end-to-end in the logarithm space. Our goal is to develop a configuration that is more effective than previous proposals, able to handle any formula, and numerically stable. To achieve this, we propose semantics that are best suited for the logarithm space and introduce novel simplifications and improvements that are crucial for optimization via gradient-descent. We use LTN as the framework for our experiments, but the conclusions of our work apply to any similar NeSy framework. Our findings, both formal and empirical, show that the proposed configuration outperforms the state-of-the-art and that each of our modifications is essential in achieving these results.

1 Introduction

Recently, there has been an increasing interest in combining logic and neural networks in Neuro-Symbolic (NeSy) integrations. The goal of such systems is often to guide the learning of neural networks using symbolic knowledge, allowing them to reason at a higher level of abstraction. Much of the recent progress in this area has focused on developing differentiable approaches for knowledge representation and reasoning.

A trend of approaches involves grounding logical symbols using neural networks and relaxing logical operators into continuous operations using fuzzy semantics. The resulting formulas, such as $\forall x \exists y P(x, y) \vee R(x)$, are associated with a truth degree in the interval $[0, 1]$ that represents their level of satisfiability. This satisfiability can then be derived with respect to the parameters of the neural

networks that ground the symbols, and is incorporated in the loss function of said neural networks to act as an additional supervision when training. In this study, we conduct experiments and analyses using Logic Tensor Networks (LTN), a well-established framework for differentiable fuzzy logics.

Previous research has highlighted that not all fuzzy operators are appropriate for this type of application. Different configurations of operators have been proposed in the literature, each with varying degrees of effectiveness, numerical stability, and applicability across different formulas. However, as of yet, no configuration has met all of these requirements simultaneously. The goal of this paper is to develop a configuration of operators that is superior to previous proposals and capable of handling any formula. To achieve this, we propose operators in the logarithm space, which is known to address certain issues. We build upon existing findings and introduce novel improvements that are crucial for optimization through gradient-descent. We call our new solution logLTN, and release it on the official github repository for LTN.¹

The foundation of the LTN framework is explained in Section 2. In Section 3, we provide an in-depth examination of the semantics in the logarithm space, with limitations in section 4. Our main contribution is in Section 3.2, which includes all the key simplifications and computational techniques, along with their formal justifications, that improve the derivability of the framework. In Section 5, we experimentally confirm that our proposition surpasses state-of-the-art configurations and, using ablation studies, that each of our modifications plays a critical role in achieving these results. Our findings are expected to help all differentiable frameworks that rely on fuzzy semantics.

2 Background on LTN

2.1 Real Logic concepts

LTN is built on Real Logic, a first-order language that allows to specify relational knowledge about the world. For example, the formula `is_friend(a,b)` states that `a` is a friend of `b`, and the formula $\forall u \forall v (\text{is_friend}(u,v) \rightarrow \text{is_friend}(v,u))$ states that `is_friend` is a symmetric relation, where u and v are variables, a and b are individuals, and `is_friend` is a predicate.

In Real Logic, a grounding \mathcal{G}_θ associates mathematical, real-valued semantics to every logical symbol depending on a set of parameters θ . Individuals are grounded with vectors of real values. Often, the vectors come from real-world features and data. A variable is grounded with a finite batch of individuals from a domain. Finally, relations are grounded using mathematical functions (generally, neural networks) that map to the truth domain $[0, 1]$.

Complex formulas are constructed using the usual logical connectives and quantifiers $\wedge, \vee, \rightarrow, \neg, \forall, \exists$. The connectives are grounded using t-norms fuzzy logic: \wedge is grounded using a t-norm T , \vee using a t-conorm S , \rightarrow using a fuzzy implication I , and \neg using a negation N . The quantifiers are grounded using aggregators A^\forall and A^\exists .

Example 1. Examples of fuzzy operators are the standard negation $N_S(x) = 1 - x$, the product t-norm $T_P(x, y) = xy$, and its dual t-conorm $S_P(x, y) = x + y - xy$. N_S is inspired by the negation of a probability. T_P is inspired by the intersection probability of two independent events. S_P is the dual t-conorm derived from the other two operators using De Morgan’s laws. For brevity, let us denote $\mathbf{x} = (x_1, \dots, x_n)$ as a vector of n values. An example of a universal aggregator is $A_{T_P}(\mathbf{x}) = \prod_{i=1}^n x_i$, which is equivalent to the conjunction of n events. Notice that all the operators function within the usual interval $[0, 1]$.

In LTN, the parameters θ are learned using *maximal satisfiability* of a knowledgebase \mathcal{K} . The satisfaction of a formula ϕ is its evaluation $\mathcal{G}_\theta(\phi)$, which returns a truth-value in $[0, 1]$. Let \mathcal{K} define a collection of formulas. The satisfaction of \mathcal{K} is defined as the aggregation of the satisfactions of each $\phi \in \mathcal{K}$. The result depends on the choice of aggregate operator, denoted by `SatAgg` (typically, the same operator as the universal aggregator).

The optimal set of parameters maximizes the objective function $\theta^* = \operatorname{argmax}_\theta \operatorname{SatAgg}_{\phi \in \mathcal{K}} \mathcal{G}_\theta(\phi)$. The following loss function is used to find that objective via gradient descent:

$$\mathcal{L}_{\text{LTN}}(\mathcal{G}_\theta, \mathcal{K}) = - \operatorname{SatAgg}_{\phi \in \mathcal{K}} \mathcal{G}_\theta(\phi) \tag{1}$$

¹<https://github.com/logictensornetworks/logictensornetworks>

For more intuition, we give a concrete example in Appendix A.1.

2.2 Appropriate Operators for Gradient Optimization

The ability to find an optimum satisfying a formula greatly depends on the choice of operators that ground the logical connectives. van Krieken *et al.* (2022) demonstrate that some fuzzy logic operators are unsuitable in a differentiable setting. For example, the Łukasiewicz t-norm $T_L(x, y) = \max(x + y - 1, 0)$ has vanishing gradients when $x + y - 1 < 0$.

The authors show that the *Product Real Logic* configuration is the most suitable for grounding the logical connectives. It uses the product t-norm, its dual t-conorm and the standard negation. For the universal aggregator, it avoids the potential underflow issues of multiplying many small numbers together by working with the log-product $(\log \circ A_{T_P})(\mathbf{x}) = \sum_{i=1}^n \log(x_i)$. Because this configuration mixes operators in the usual and logarithm spaces, it has limitations in expressivity and cannot handle certain formulas (e.g. $(\forall u P(u)) \vee (\forall v Q(v))$). We discuss this further in Appendix A.2.

In this paper, we aim to explore a configuration that 1) performs better than Product Real Logic, 2) can handle any formula, and 3) is numerically stable.

3 Introducing logLTN

We present logLTN, a specification of LTN with end-to-end semantics in the logarithm space. Section 3.1 introduces operators that can manipulate appropriately log truth degrees. Section 3.2 shows how to modify these operators to perform well in a differentiable setting.

3.1 Semantics

We employ the product t-norm $T_P(x, y) = xy$ and the maximum t-conorm $S_M(x, y) = \max(x, y)$. These operators are known to simplify easily in the logarithm space and are commonly used in the log probability literature. We also use the standard negation operator $N_S(1 - x)$. Implications are replaced using the material implication rule $(\phi \rightarrow \psi) \equiv (\neg\phi \vee \psi)$, which means we rewrite every implication using $I(x, y) = S(N(x), y)$.

The universal aggregator is defined as the conjunction of n events $A_{T_P}(\mathbf{x}) = \prod_{i=1}^n x_i$, and the existential aggregator is defined as the disjunction of n events $A_{S_M}(\mathbf{x}) = \max_{i=1}^n(x_i)$.

3.1.1 Logarithm space

We denote $(\log \circ \mathcal{G}_\theta)(\phi)$ as the log-grounding of a formula and $(\log \circ \text{FuzzyOp})$ as the log-grounding of an operator. Note that maximizing the log grounding of a formula is equivalent to maximizing its grounding as logarithms are monotone increasing functions. The log-grounding of T_P , S_M , and their generalizations in aggregators, simplify easily.

$$(\log \circ T_P)(x, y) = \log(x) + \log(y) \quad (2)$$

$$(\log \circ S_M)(x, y) = \max(\log(x), \log(y)) \quad (3)$$

$$(\log \circ A_{T_P})(\mathbf{x}) = \sum_{i=1}^n \log(x_i) \quad (4)$$

$$(\log \circ A_{S_M})(\mathbf{x}) = \max_{i=1}^n(\log(x_i)) \quad (5)$$

Expressing $\log \circ N_S(x)$ as a function with a logarithmic input requires the computation of an exponent and a logarithm. This means that the operator cannot easily take an input in the logarithm space, for example, in $\neg(A \wedge B)$. To overcome this, we write formulas in *negative normal form* (NNF). A formula is in NNF when the scope of each negation operator only applies to atoms (predicates), not to complex formulas, and when the formula does not contain any implication or equivalence symbols. For example, if A and B are two atoms, $\neg A \wedge \neg B$ is in NNF but $\neg(A \vee B)$ is not.

3.2 Optimizing in logLTN

3.2.1 Numerical stability of log negations

Let $f(x)$ be the output of a neural predicate in the interval $[0, 1]$ depending on a mathematical variable x . Converting a value to the logarithm space is a risky operation in a computational graph, as both $\log(f(x))$ and $\frac{\partial \log(f(x))}{\partial x} = \frac{1}{f(x)} \frac{\partial f(x)}{\partial x}$ can cause overflow errors when $f(x)$ tends to 0.

In NeSy AI, predicates are typically grounded using a final sigmoid or softmax layer to normalize outputs in $[0, 1]$. Fortunately, the computation and differentiation of the logarithm of a sigmoid or softmax simplifies to a stable expression (refer to Appendix A.3). For this reason, most frameworks for automatic differentiation, such as TensorFlow or PyTorch, offer built-in and all-in-one layer implementations of the log sigmoid and log softmax functions. These should be used when log-grounding a predicate to avoid unstable gradients.

However, the same issue arises when log-grounding the negation of a predicate, $\log(1 - f(x))$. Fortunately, we show how to reformulate the log-negation of a sigmoid or softmax predicate to numerically stable expressions.

Theorem 1. *The log-negation of a sigmoid function $S(x) = \frac{1}{1+e^{-x}}$, $x \in \mathbb{R}$, simplifies as*

$$(\log \circ N_S)(S(x)) = \log(S(x)) - x \quad (6)$$

Proof. Proof in Appendix C.1.1. □

Theorem 2. *The log-negation of a softmax function $\sigma(\mathbf{z})_i = \frac{e^{z_i}}{\sum_{j=1}^K e^{z_j}}$, where $\mathbf{z} = (z_1, \dots, z_K) \in \mathbb{R}^K$ is a vector of K real values, and $i = 1, \dots, K$, simplifies as*

$$(\log \circ N_S)(\sigma(\mathbf{z})_i) = \log(\sigma(\mathbf{z})_i) + \log \left(\sum_{\substack{j=1 \\ j \neq i}}^K e^{z_j} \right) - z_i \quad (7)$$

Proof. Proof in Appendix C.1.2. □

These two proposed reformulations have numerically stable implementations. The first uses the logarithm of a sigmoid and a linear term. The second uses the logarithm of a softmax function, a linear term, and a logarithm of a sum of exponentials, also known as LogSumExp. LogSumExp also has a stable implementation and its derivative is a softmax function.

Below, we briefly show the stability advantage of our reformulation for sigmoid by comparing its output with a naive definition $\log(1 - S(x))$. The results are obtained in TensorFlow with float32 precision. The same can be reproduced with the softmax reformulation.

```

Input :
  x : [0., 10., 100., 1000., 10000.]
Output :
  f1(x)=log(1-S(x)) : [-0.69, -1.0e+1, -inf, -inf, -inf]
  df1/dx(x)         : [-0.5, -1.0, nan, nan, nan]
  f2(x)=log(S(x))-x : [-0.69, -1.0e+1, -1.0e+2, -1.0e+3, -1.0e+4]
  df2/dx(x)         : [-0.5, -1.0, -1.0, -1.0, -1.0]

```

3.2.2 Relaxation of the disjunctions

The maximum operator in equations (3) and (5) is unsuitable in a differentiable setting as it has single-passing gradients. This means that it only propagates gradients to one input at a time, the one with the highest value. Intuitively, let the formula $\exists x P(x)$ be a constraint used to optimize a neural predictor P . If several individuals in the batch x tend to verify $P(x)$, max will have non-zero gradients for only one of them. This can be inefficient in practice as it will push the predictor to overfit that single individual in x and ignore the others. Also, it is particularly sensitive to initial conditions.

A common solution is to use a smooth approximation of the maximum operator. A popular candidate in the logarithm space is the LogSumExp (LSE) operator, defined as:

$$\text{LSE}(\mathbf{x} \mid \alpha, C) = \frac{1}{\alpha} \left(C + \log \left(\sum_{i=1}^n e^{\alpha x_i - C} \right) \right) \quad (8)$$

(9)

$C = \max(\alpha \mathbf{x})$ is a constant that does not change the result of the expression but prevents overflow errors in the exponential terms. α is a hyperparameter that scales the bounds of LSE according to the following inequality:

$$\max(\mathbf{x}) \leq \text{LSE}(\mathbf{x} \mid \alpha, C) \leq \max(\mathbf{x}) + \frac{\log(n)}{\alpha} \quad (10)$$

Here, we identify an issue in that LogSumExp approaches the maximum value via a higher bound. This is problematic, as truth degrees are bound to the interval $[0, 1]$, and log truth degrees should be bound in the interval $[-\infty, 0]$.² With LSE, the output of a log-disjunction can exceed these bounds and become non-negative.

To address this issue, we propose the use of a LogMeanExp operator LME:

$$\text{LME}(\mathbf{x} \mid \alpha, C) = \frac{1}{\alpha} \left(C + \log \left(\frac{\sum_{i=1}^n e^{\alpha x_i - C}}{n} \right) \right) \quad (11)$$

It approaches the maximum operator from below values (proof in Appendix C.2.1):

$$\max(\mathbf{x}) - \frac{\log(n)}{\alpha} \leq \text{LME}(\mathbf{x} \mid \alpha, C) \leq \max(\mathbf{x}) \quad (12)$$

This operator is numerically stable, well-bounded, and suitable for derivation. We use it to ground disjunctions and existential quantifications in logLTN. For best practice, the parameter α that scales the smooth maximum should be scheduled over time to balance exploration and exploitation Badreddine *et al.* (2022).

3.2.3 Batch-size invariance for the universal aggregation

We have improved the derivability of negations, disjunctions, and existential quantifiers in the logarithm space. Here, we identify an issue with the universal quantification.

Consider a knowledge base with two rules $\phi_1 = \forall u P(u)$ and $\phi_2 = \exists v Q(v)$. Let $\mathcal{G}(u) = [x_1, \dots, x_m]$ and $\mathcal{G}(v) = [y_1, \dots, y_n]$ be two batches of individuals. Let us develop the groundings of the rules:

$$(\log \circ \mathcal{G}_\theta)(\phi_1) = \sum_{i=1}^m (\log \circ \mathcal{G}_\theta)(P)(x_i) \quad (13)$$

$$(\log \circ \mathcal{G}_\theta)(\phi_2) = \max_{i=1}^n (\log \circ \mathcal{G}_\theta)(Q)(y_i) \quad (14)$$

In the loss $\mathcal{L} = -(\log \circ \mathcal{G}_\theta)(\phi_1 \wedge \phi_2) = -(\log \circ \mathcal{G}_\theta)(\phi_1) - (\log \circ \mathcal{G}_\theta)(\phi_2)$, the optimization will tend to overfit the rule with the universal quantifier and ignore the existential rule for large batch sizes. This is due to the fact that the first sums m log truth degrees, whereas the second only takes one log truth degree as a maximum. In terms of differentiability, the universal rule weights more on the gradient updates, as $\sum_{i=1}^m \frac{\partial \mathcal{L}}{\partial \log \circ \mathcal{G}_\theta(P)(x_i)} = \sum_{i=1}^m -1 = -m$, whereas $\sum_{i=1}^n \frac{\partial \mathcal{L}}{\partial \log \circ \mathcal{G}_\theta(Q)(y_i)} = \sum_{i=1}^n -\delta_{ij} = -1$ given $j = \text{argmax}_{j=1}^n \mathcal{G}_\theta(Q)(y_j)$. The problem remains with the smooth maximum LogMeanExp, whose gradients are a softmax function summing to 1 as well.

This weighing problem can also arise when comparing two universal quantifiers, such as $\forall u P(u)$ and $\forall v Q(v)$. If the batches for u and v have varying sizes, the optimization algorithm will tend to overfit the rule that has more examples of individuals and ignore the other.

²The edge case $\log(0) = -\infty$ can be avoided by add a small real value $\varepsilon > 0$ to zero truth degrees. However, this is rarely a problem in practice as sigmoid and softmax layers output values in $]0, 1[$.

To solve this problem, we propose to use a mean instead of a sum as a weighting scheme to balance universal quantifiers:

$$(\log \circ \mathcal{G})(\forall u P(u)) = \sum_{i=1}^m \frac{(\log \circ \mathcal{G})(P)(x_i)}{m} \quad (15)$$

By averaging log truth degrees instead of summing them, we obtain a *batch-size invariant* aggregator. The weight of the gradients becomes $\sum_{i=1}^m \frac{\partial \mathcal{L}}{\partial \log \circ \mathcal{G}(P)(x_i)} = -1$. This ensures every formula weighs equally in the loss function.

In the normal space, the universal quantifiers then correspond to geometric means instead of products. This trick alters the objective and search space of the task, but we find that it is crucial to approach good solutions in our experiments.

3.2.4 Summary

By implementing all the aforementioned modifications, we arrive at the log-grounding routine presented in Algorithm 1.

Algorithm 1 Compute $(\log \circ \mathcal{G}_\theta)(\phi)$ for derivability

- 1: **Step 1** Rewrite ϕ in negative normal form
 - 2: **Step 2** Log-ground predicates and their negations
 - 3: Use the log-negation simplifications with sigmoid/softmax layers (Equations 6 and 7)
 - 4: **Step 3** Compute connectives in the logarithm space
 - 5: \wedge becomes +
 - 6: \vee becomes LME
 - 7: \forall becomes mean
 - 8: \exists becomes LME
-

4 Limitations

4.1 De Morgan’s Laws and NNF

The Negative Normal Form (NNF) does not preserve equivalence with the logarithmic semantics introduced in Section 3.1. To transform a formula in NNF, one must push the negations in front of atoms using De Morgan’s laws, but the laws do not hold given that $T_P(x, y) = xy$ and $S_M(x, y) = \max(x, y)$ are not fuzzy dual operators. However, we can prove the following De Morgan’s inequalities:

Theorem 3. Let P and Q be two formulas. We can show that

$$\mathcal{G}(\neg(P \wedge Q)) \geq \mathcal{G}(\neg P \vee \neg Q) \quad (16)$$

$$\mathcal{G}(\neg(P \vee Q)) \geq \mathcal{G}(\neg P \wedge \neg Q) \quad (17)$$

$$\mathcal{G}(\neg(\forall u P(u))) \geq \mathcal{G}(\exists u \neg P(u)) \quad (18)$$

$$\mathcal{G}(\neg(\exists u P(u))) \geq \mathcal{G}(\forall u \neg P(u)) \quad (19)$$

Proof. Proof in Appendix C.3.1. □

These results stem from the fact that $\max(x, y)$ is a lower-bound to other t-conorms including the dual product t-conorm. In Appendix C.3.2, we analyze the tightness of these bounds. Given that NNF is obtained by repeatedly applying De Morgan’s laws, we can infer the following property:

Corollary 3.1. Let ϕ be any formula and ϕ' be a NNF formula derived syntactically from ϕ using De Morgan’s laws. Then, $\mathcal{G}_\theta(\phi') \leq \mathcal{G}_\theta(\phi)$, meaning that the satisfaction of the NNF formula ϕ' is a lower bound for the satisfaction of the formula ϕ .

This is particularly useful as, if we convert a formula into NNF and find a parametric grounding that satisfies it, we know that the original formula is at least as satisfied.

5 Experiments

5.1 Task 1: Clustering

The first experiment is a clustering problem based on the gene expression cancer RNA-Seq benchmark from the UCI ML datasets repository Dua & Graff (2017). The dataset has 801 samples of 20531 features, which we reduce to 16 features using PCA. The task is to divide samples into five clusters, which roughly correspond with five ground truth cancer types. We train a neural predictor $C(x, c)$ that returns the belief of a point x belonging in a given cluster c using these three constraints:

$$\forall x \exists c C(x, c) \quad (20)$$





$$\forall c \exists x C(x, c) \quad (21)$$

$$\forall (c, x, y : |x - y| < \text{th}_{2.5}) C(x, c) \rightarrow C(y, c) \quad (22)$$

x and y are grounded with the batch of 801 points. c is a variable that ranges over five cluster ids. $C(x, c)$ outputs beliefs using a softmax output layer that ensures mutual exclusivity of clusters. (22) uses the concept of "guarded quantification" introduced by Badreddine *et al.* (2022). It means that the quantification only retains the individuals verifying the condition $|x - y| < \text{th}_{2.5}$, where $\text{th}_{2.5}$ is the 2.5-th percentile of the euclidean distances between all pairs of points. Intuitively, the constraint states that for any pair of points that are very close, if one belongs to a cluster, the other must belong in the same cluster.

We use this task, inspired by the toy example from Badreddine *et al.* (2022) and extended on real-world data, as it is one of the rare NeSy tasks with existential clauses ranging over many individuals (here, 801 individuals).

5.2 Task 2: MNISTAdd

The second problem is the MNISTAdd task from Manhaeve *et al.* (2018). We experiment on the 2-digits number variant of the task. In this problem, we learn to recognize the sum of two numbers of two digits using only the result of the sum as a training label. For example, a dataset sample would be (, , , , 130).

The task is modeled using a digit classifier $\text{is_digit}(x, d)$ which predicts beliefs for the MNIST image being the digit $d = 0 \dots 9$. Whereas we only provide labels for the final result of the addition, NeSy methods use prior knowledge about intermediate labels (possible digits used in the addition) to propagate ground truth information to the digit classifier. Given the MNIST images and sum result $([x_1, x_2], [y_1, y_2], n)$, we use the LTN constraint from Badreddine *et al.* (2022):

$$\begin{aligned} \exists d_1, d_2, d_3, d_4 : 10d_1 + d_2 + 10d_3 + d_4 = n \\ (\text{is_digit}(x_1, d_1) \wedge \text{is_digit}(x_2, d_2) \wedge \text{is_digit}(y_1, d_3) \wedge \text{is_digit}(y_2, d_4)) \end{aligned} \quad (23)$$

The loss signal is a universal aggregation of the constraint over minibatches of labeled examples. We use the same neural network for is_digit as Manhaeve *et al.* (2018). This is a basic experiment with a single training constraint. We assess it because many probabilistic NeSy methods use it as a standard for comparison.

5.3 Task 3: Semantic PASCAL-Part

The third experiment is a semi-supervised semantic image interpretation task on the semantic PASCAL-Part dataset from Donadello *et al.* (2017). The goal is to train a type classifier $\text{is}(x, \text{bottle})$, $\text{is}(x, \text{cap})$, etc., that predicts the type of an object within a bounding box x , and to train a relation predictor $\text{partOf}(x, y)$ that determines if one bounding box x is part of another bounding box y . An example of such bounding boxes is presented in Figure 1.

Training is guided by three constraints based on ground truth examples, one for labeled type examples, one for pairs of positive examples for partOf , and one for pairs of negative examples. The ground truth labels are made available for only 5% of the training data. However, training is carried on the unlabeled data using mereological constraints that relate to the types and their meanings, for example:

$$\forall x, y \text{ is}(x, \text{bottle}) \wedge \text{partOf}(y, x) \rightarrow (\text{is}(y, \text{cap}) \vee \text{is}(x, \text{body})) \quad (24)$$

$$\forall x, y \text{ is}(x, \text{cap}) \wedge \text{partOf}(x, y) \rightarrow \text{is}(y, \text{bottle}) \quad (25)$$

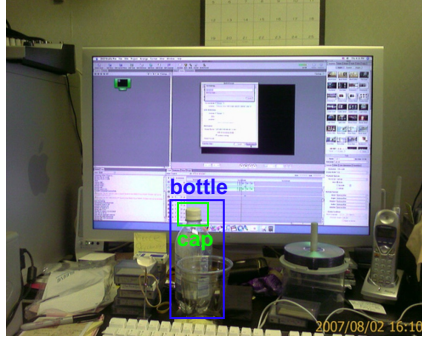


Figure 1: Example of bounding boxes from PASCAL-Part.

Donadello *et al.* (2017) grounded the bounding boxes using predictions produced by an object detector trained on PASCAL-Part. This means that LTN was only used to correct the predictions of the detector. We increase the difficulty of the task by implementing the bounding boxes with a latent vector of 1024 features output by a pre-trained FasterRCNN backbone. That is, LTN has to learn all the final layers of the object detector and its specialization on PASCAL-Part. We release our version of the dataset on <https://github.com/sbadredd/semantic-pascal-part>. More details on the experiment are available in Appendix B.1.

Out of the three tasks, this is by far the largest with a total 59 object types and 60 corresponding constraints. It showcases the power of LTN and its capability to simply integrate many constraints in a loss function. We evaluate the type classification using balanced accuracy, $\text{partOf}(x, y)$ using the area under precision-recall curves, and the semantic interpretation by reporting the number of false positives that violate the mereological constraints – for example, a bottle is predicted to be part of a cap.

5.4 Baselines

We compare logLTN with the following baselines. Note that we skip the ablation of the log-negation simplifications, as their numerical practicability is already illustrated in Section 3.2.1.

LTN-Prod Product Real Logic was identified by van Krieken *et al.* (2022) as the best performing operator semantics for differentiable fuzzy logics. It uses the product t-norm $T_P(x, y) = xy$ and its dual t-conorm $S_P(x, y) = x + y - xy$. The universal quantifier uses the log-product aggregator $(\log \circ A_{T_P})(\mathbf{x}) = \sum_{i=1}^n \log(x_i)$ and the existential quantifier uses a smooth maximum. Its combination of operators both in the usual and logarithm space makes it difficult to handle certain formulas. We discuss this issue further in appendix A.2.

LTN-Stable Stable Product Real Logic Badreddine *et al.* (2022) is a modification of LTN-Prod that uses a smooth minimum for the universal aggregator, such that all operators perform in the usual space. A limitation of the smooth minimum is that it depends on a smoothing hyperparameter p , which we show to greatly influence the results.

logLTN the configuration introduced in this paper, performing fully in the logarithm space.

logLTN-sum an ablation of logLTN using a sum instead of a batch-size invariant mean for universal aggregations. See Section 3.2.3

logLTN-max an ablation logLTN that uses a non-relaxed maximum operator for existential aggregations. See Section 3.2.2.

logLTN-LSE an ablation of logLTN that uses a traditional LogSumExp operator for existential aggregations instead of LogMeanExp. See Section 3.2.2.

6 Results

The code for our experiments is available at <https://github.com/sbadredd/logltn-experiments>. We perform experiments with runs of 1000 training steps for the clustering problem, runs of 20 epochs for

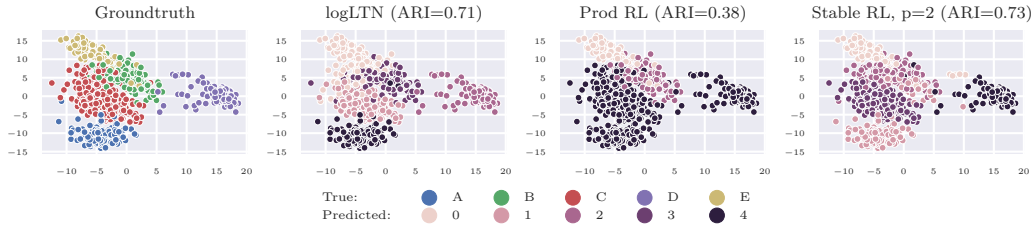


Figure 2: 2D PCA plots of typical cluster assignments by each baseline

MNISTAdd with two different dataset sizes, and runs of 1000 training steps for Semantic PASCAL-Part. The results are summarized in Tables 1 and 3. Because Semantic PASCAL-Part is more computationally demanding, we conducted ablation studies only on the two first experiments. For additional implementation details, please refer to Appendix B.2 covering training configuration and baseline hyperparameters. Across all metrics, logLTN consistently achieved the best or second best performance.

LTN-Prod performs poorly in the clustering task. In a qualitative analysis of the cluster assignments (Figure 2), we observe that LTN-Prod disregards constraint (21) stating that each cluster contains at least one point. This is due to the batch-variant log-product. As that constraint is quantified over five clusters ($\forall c$), it has relatively less weight compared to the other ones aggregated over all points. Also, in Semantic PASCAL-Part, while LTN-Prod exhibits good results, logLTN still demonstrates superior performance by avoiding on average 34% more mereological violations and having less deviation across all metrics than LTN-Prod.

We tested LTN-Stable with the smooth minimum parameter $p = 2$ and $p = 6$. When $p = 2$, the smooth minimum is less strict and corresponds to a Mean-Squared Error (MSE) aggregator. This leads to low accuracy in the PASCAL-Part problem, as the constraint aggregator focuses on satisfying the 57 logical constraints rather than the three ground truth constraints which it treats as "outliers". The result is a predictor classifying all objects into barely constrained types (e.g. background) and all partOf(x, y) as false negatives in order to reach low mereological violations. With $p = 6$, the aggregator is more strict but can overfit outliers and exhibit instability in other experiments. Despite its name, we find LTN-Stable to be too dependent on the hyperparameter p and unstable.

Regarding the ablations, logLTN-max generally performed poorly due to inadequate gradient propagation. logLTN-LSE showed similar performance to logLTN overall, except for deviating results in MNISTAdd, possibly due to the unbounded maximum breaking at an edge case. Also, even on well-performing problems, we find that grounding the knowledgebase with logLTN-LSE can lead to log truth degrees reaching values as high as $(\log \circ \mathcal{G})(\mathcal{K}) = 5$. That corresponds to a truth degree of approximately $(\log \circ \mathcal{G})(\mathcal{K}) = 150$. Since fuzzy truth degrees should be within the range of $[0, 1]$, the higher values generated by logLTN-LSE make it unusable in many cases, making logLTN a more suitable option.

Finally, logLTN-sum exhibits behavior akin to LTN-Prod in clustering due to its batch-variant aggregator. In MNISTAdd, logLTN-sum outperforms logLTN, but the only difference between the two baselines is a constant factor in the loss function due to taking a mean over the minibatch of samples instead of a sum. We assume that scaling the learning rate accordingly would yield comparable results with logLTN.

In Table 2, we compare our MNISTAdd results with those reported by popular probabilistic frameworks Manhaeve *et al.* (2018); Winters *et al.* (2022); Pryor *et al.* (2022). In their study, Badreddine *et al.* (2022) showed that LTN managed to solve the MNISTAdd problem, but the outcomes varied significantly due to instability during initialization. We show that by training with logLTN in the logarithm space, we resolved this issue and achieved standard state-of-the-art performance in the task.

	Clustering	MNISTAdd	
		1,500 samples	15,000 samples
LTN-Prod	0.37 ± 0.18	$88.39 \pm 0.97^*$	95.39 ± 0.33
LTN-Stable (p=2)	0.71 ± 0.10	62.77 ± 37.16	80.34 ± 32.82
LTN-Stable (p=6)	0.62 ± 0.05	30.51 ± 34.19	95.12 ± 0.62
logLTN	$0.71 \pm 0.06^*$	88.29 ± 0.78	$95.61 \pm 0.51^*$
logLTN-LSE	0.72 ± 0.05	75.35 ± 29.96	95.27 ± 0.53
logLTN-max	0.35 ± 0.17	48.39 ± 36.80	80.81 ± 32.64
logLTN-sum	0.36 ± 0.22	88.49 ± 0.88	95.62 ± 0.42

Table 1: Results on Clustering (Adjusted Rand Index scores – averaged on 10 runs) and MNISTAdd (test accuracy – averaged on 5 runs).

	1,500 samples	15,000 samples
DeepProbLog	$87.21 \pm 1.92^*$	95.16 ± 1.70
DeepStochLog	NA	96.40 ± 0.10
NeuPSL	87.05 ± 1.48	93.91 ± 0.37
logLTN	88.29 ± 0.78	$95.61 \pm 0.51^*$

Table 2: Reported test accuracy on MNISTAdd by probabilistic baselines. DeepStochLog does not report results on the training set size 1,500.

7 Related Work

The field of combining logic and neural networks in NeSy integrations is gaining interest, as outlined by Garcez & Lamb (2020). For an overview of the approaches and challenges, see Hitzler & Sarker (2022). To understand the prevalence of these systems, refer to Sarker *et al.* (2021).

A family of approaches converts logical connectives into differentiable operations using fuzzy semantics. Systems that employ this approach include LTN Serafini & d’Avila Garcez (2016); Badreddine *et al.* (2022), KALE Guo *et al.* (2016), SBR Diligenti *et al.* (2017), and LRNN Sourek *et al.* (2018) among others. Unlike probabilistic logics Manhaeve *et al.* (2018); Winters *et al.* (2022), fuzzy approaches change logic semantics and are less common in proof reasoning. Nevertheless, fuzzy frameworks excel in knowledge-aided learning and offer simplicity compared to probabilistic methods which must often solve the exponentially complex model counting problem.

Fuzzy frameworks have been used in a wide range of applications and fields in recent years. These include but are not limited to semantic image interpretation Donadello *et al.* (2017), natural language processing Bianchi *et al.* (2019), reinforcement learning Badreddine & Spranger (2019), query answering over knowledge graphs Arakelyan *et al.* (2021); Chen *et al.* (2022), or open-world reasoning Wagner & d’Avila Garcez (2022). Our paper aligns with the research stream of van Krieken *et al.* (2022) as it strives to improve the performance of all these related works by providing mathematical and computational cues for fuzzy semantics.

8 Conclusions

Many NeSy approaches rely on fuzzy operator semantics to ground knowledge in loss functions. However, it is clear that not all semantics are suitable for gradient descent optimization algorithms.

	PartOf AUC	Type Accuracy	# Mereological Violations
LTN-Prod	71.38 ± 10.38	$53.40 \pm 1.81^*$	$16,312.8 \pm 4,180.2$
LTN-Stable (p=2)	18.62 ± 28.16	1.90 ± 0.46	$1,196.0 \pm 2,674.3$
LTN-Stable (p=6)	64.85 ± 3.05	34.53 ± 1.62	$24,324.5 \pm 14,052.3$
logLTN	$69.57 \pm 4.33^*$	55.54 ± 1.00	$10,708.2 \pm 1,455.9^*$

Table 3: Test results on Semantic PASCAL-Part averaged on 5 runs.

In this paper, we propose a set of semantics that can be used to train logic end-to-end in the logarithm space. We demonstrate that the proposed configuration outperforms semantics previously considered state-of-the-art in such NeSy systems.

We propose the solution, which we refer to as logLTN, as an additional set of semantics for LTN and implement it in the repository of the framework. Each of our findings can also be applied separately to any framework that works with logic in the logarithm space. In summary, our recommendations for such systems include computing log-negations using Equations (6) and (7), relaxing disjunctions using Equation (11), and making universal quantifications batch size-invariant using Equation (15). Our research is expected to improve the performance of all NeSy approaches that rely on fuzzy operator semantics.

References

- Arakelyan, Erik, Daza, Daniel, Minervini, Pasquale, & Cochez, Michael. 2021. Complex Query Answering with Neural Link Predictors. *In: 9th International Conference on Learning Representations, ICLR 2021, Virtual Event, Austria, May 3-7, 2021*. OpenReview.net.
- Badreddine, Samy, & Spranger, Michael. 2019. Injecting Prior Knowledge for Transfer Learning into Reinforcement Learning Algorithms using Logic Tensor Networks. *In: Doran, Derek, d'Avila Garcez, Artur S., & Lécué, Freddy (eds), Proceedings of the 2019 International Workshop on Neural-Symbolic Learning and Reasoning (NeSy 2019), Annual workshop of the Neural-Symbolic Learning and Reasoning Association, Macao, China, August 12, 2019*.
- Badreddine, Samy, d'Avila Garcez, Artur, Serafini, Luciano, & Spranger, Michael. 2022. Logic Tensor Networks. *Artificial Intelligence*, **303**(Feb.), 103649.
- Bianchi, Federico, Palmonari, Matteo, Hitzler, Pascal, & Serafini, Luciano. 2019. Complementing Logical Reasoning with Sub-symbolic Commonsense. *Pages 161–170 of: Fodor, Paul, Montali, Marco, Calvanese, Diego, & Roman, Dumitru (eds), Rules and Reasoning*. Lecture Notes in Computer Science. Cham: Springer International Publishing.
- Chen, Xianjie, Mottaghi, Roozbeh, Liu, Xiaobai, Fidler, Sanja, Urtasun, Raquel, & Yuille, Alan L. 2014. Detect What You Can: Detecting and Representing Objects Using Holistic Models and Body Parts. *Pages 1979–1986 of: 2014 IEEE Conference on Computer Vision and Pattern Recognition, CVPR 2014, Columbus, OH, USA, June 23-28, 2014*. IEEE Computer Society.
- Chen, Xuelu, Hu, Ziniu, & Sun, Yizhou. 2022. Fuzzy Logic Based Logical Query Answering on Knowledge Graphs. *Proceedings of the AAAI Conference on Artificial Intelligence*, **36**(4), 3939–3948.
- Diligenti, Michelangelo, Roychowdhury, Soumali, & Gori, Marco. 2017. Integrating Prior Knowledge into Deep Learning. *Pages 920–923 of: 2017 16th IEEE International Conference on Machine Learning and Applications (ICMLA)*. Cancun, Mexico: IEEE.
- Donadello, Ivan, Serafini, Luciano, & d'Avila Garcez, Artur S. 2017. Logic Tensor Networks for Semantic Image Interpretation. *Pages 1596–1602 of: Sierra, Carles (ed), Proceedings of the Twenty-Sixth International Joint Conference on Artificial Intelligence, IJCAI 2017, Melbourne, Australia, August 19-25, 2017*. ijcai.org.
- Dua, Dheeru, & Graff, Casey. 2017. *UCI Machine Learning Repository*.
- Garcez, Artur d'Avila, & Lamb, Luis C. 2020 (Dec.). *Neurosymbolic AI: The 3rd Wave*. arXiv:2012.05876 [cs].
- Guo, Shu, Wang, Quan, Wang, Lihong, Wang, Bin, & Guo, Li. 2016. Jointly Embedding Knowledge Graphs and Logical Rules. *Pages 192–202 of: Su, Jian, Carreras, Xavier, & Duh, Kevin (eds), Proceedings of the 2016 Conference on Empirical Methods in Natural Language Processing, EMNLP 2016, Austin, Texas, USA, November 1-4, 2016*. The Association for Computational Linguistics.
- Hitzler, P., & Sarker, M.K. 2022. *Neuro-symbolic Artificial Intelligence: The State of the Art*. Frontiers in artificial intelligence and applications. IOS Press.

- Manhaeve, Robin, Dumancic, Sebastijan, Kimmig, Angelika, Demeester, Thomas, & De Raedt, Luc. 2018. DeepProbLog: Neural Probabilistic Logic Programming. *In: Bengio, S., Wallach, H., Larochelle, H., Grauman, K., Cesa-Bianchi, N., & Garnett, R. (eds), Advances in Neural Information Processing Systems*, vol. 31. Curran Associates, Inc.
- Manigrasso, Francesco, Miro, Filomeno Davide, Morra, Lia, & Lamberti, Fabrizio. 2021. Faster-LTN: a neuro-symbolic, end-to-end object detection architecture. *CoRR*, **abs/2107.01877**.
- Pryor, Connor, Dickens, Charles, Augustine, Eriq, Albalak, Alon, Wang, William, & Getoor, Lise. 2022. *NeuPSL: Neural Probabilistic Soft Logic*.
- Ren, Shaoqing, He, Kaiming, Girshick, Ross B., & Sun, Jian. 2017. Faster R-CNN: Towards Real-Time Object Detection with Region Proposal Networks. *IEEE Trans. Pattern Anal. Mach. Intell.*, **39**(6), 1137–1149.
- Sarker, Md. Kamruzzaman, Zhou, Lu, Eberhart, Aaron, & Hitzler, Pascal. 2021. Neuro-Symbolic Artificial Intelligence: Current Trends. *CoRR*, **abs/2105.05330**.
- Serafini, Luciano, & d’Avila Garcez, Artur S. 2016. Logic Tensor Networks: Deep Learning and Logical Reasoning from Data and Knowledge. *In: Besold, Tarek R., Lamb, Luís C., Serafini, Luciano, & Tabor, Whitney (eds), Proceedings of the 11th International Workshop on Neural-Symbolic Learning and Reasoning (NeSy’16) co-located with the Joint Multi-Conference on Human-Level Artificial Intelligence (HLAI 2016), New York City, NY, USA, July 16-17, 2016*. CEUR Workshop Proceedings, vol. 1768. CEUR-WS.org.
- Sourek, Gustav, Aschenbrenner, Vojtech, Zelezny, Filip, Schockaert, Steven, & Kuzelka, Ondrej. 2018. Lifted Relational Neural Networks: Efficient Learning of Latent Relational Structures. *Journal of Artificial Intelligence Research*, **62**(May), 69–100.
- van Krieken, Emile, Acar, Erman, & van Harmelen, Frank. 2019. Semi-supervised Learning using Differentiable Reasoning. *FLAP*, **6**(4), 633–652.
- van Krieken, Emile, Acar, Erman, & van Harmelen, Frank. 2022. Analyzing Differentiable Fuzzy Logic Operators. *Artificial Intelligence*, **302**(Jan.), 103602.
- Wagner, Benedikt, & d’Avila Garcez, Artur S. 2022. Neural-Symbolic Reasoning Under Open-World and Closed-World Assumptions. *In: Martin, Andreas, Hinkelmann, Knut, Fill, Hans-Georg, Gerber, Aurora, Lenat, Doug, Stolle, Reinhard, & van Harmelen, Frank (eds), Proceedings of the AAAI 2022 Spring Symposium on Machine Learning and Knowledge Engineering for Hybrid Intelligence (AAAI-MAKE 2022), Stanford University, Palo Alto, California, USA, March 21-23, 2022*. CEUR Workshop Proceedings, vol. 3121. CEUR-WS.org.
- Winters, Thomas, Marra, Giuseppe, Manhaeve, Robin, & Raedt, Luc De. 2022. DeepStochLog: Neural Stochastic Logic Programming. *Proceedings of the AAAI Conference on Artificial Intelligence*, **36**(9), 10090–10100. Number: 9.

A Background

A.1 LTN Example

Let us denote the predicate `is_friend` as `f` for brevity. In the expression `f(a, b)`, let $\mathcal{G}_\theta(a)$ and $\mathcal{G}_\theta(b)$ be vector embeddings in \mathbb{R}^m . A primitive approximation of the friendship relationship could be a cosine similarity function $\mathcal{G}_\theta(f) : (\mathbf{x}, \mathbf{y}) \mapsto \frac{\mathbf{x} \cdot \mathbf{y}}{\|\mathbf{x}\| \|\mathbf{y}\|}$. If $\mathcal{G}_\theta(a) = [3 \ 2 \ 0 \ 5]$ and $\mathcal{G}_\theta(b) = [1 \ 0 \ 0 \ 4]$, we have $\mathcal{G}_\theta(f(a, b)) = 0.905$; that is, a high truth degree.

Of course, stating that people are friends if they are similar is primitive. In a real-case scenario, the friendship relationship would likely be approximated by a parametric function, such as a neural network, and trained based on constraints in a loss function.

Consider the formula $\phi = \neg f(a, b) \vee f(b, a)$ and a knowledgebase that contains this unique formula $\mathcal{K} = \{\phi\}$. The formula states that if `a` is a friend of `b`, then `b` is a friend of `a`.³ Let the grounding for $\mathcal{G}_\theta(f(a, b))$ depend on a trainable neural network for the friendship relation and a set of features for `a` and `b`. To update θ via gradient descent steps, we calculate $\frac{\partial \mathcal{G}_\theta(\phi)}{\partial \mathcal{G}_\theta(f(a, b))}$ and $\frac{\partial \mathcal{G}_\theta(\phi)}{\partial \mathcal{G}_\theta(f(b, a))}$. Using the operators $N_S(x) = 1 - x$ and $S_P(x, y) = x + y - xy$, we get:

$$\mathcal{G}_\theta(\phi) = S_P(N_S(\mathcal{G}_\theta(f(a, b))), \mathcal{G}_\theta(f(b, a))) \quad (26)$$

$$= 1 - \mathcal{G}_\theta(f(a, b)) + \mathcal{G}_\theta(f(a, b))\mathcal{G}_\theta(f(b, a)) \quad (27)$$

And the partial derivatives:

$$\frac{\partial \mathcal{G}_\theta(\phi)}{\partial \mathcal{G}_\theta(f(b, a))} = \mathcal{G}_\theta(f(a, b)) \quad (28)$$

$$\frac{\partial \mathcal{G}_\theta(\phi)}{\partial \mathcal{G}_\theta(f(a, b))} = -1 + \mathcal{G}_\theta(f(b, a)) \quad (29)$$

Equations (29) and (28) give us interesting insights on the power of LTN. When maximizing the satisfiability of the formula, if `f(a, b)` is high, then $\frac{\partial \mathcal{G}_\theta(\phi)}{\partial \mathcal{G}_\theta(f(b, a))}$ is high. Intuitively, if `a` being friend with `b` has a high truth value, LTN will tend to increase the truth value of `b` being friend with `a`. Alternatively, if `f(b, a)` is low, $\frac{\partial \mathcal{G}_\theta(\phi)}{\partial \mathcal{G}_\theta(f(a, b))}$ is close to -1 . That means that if `b` is not considered friend with `a`, LTN will tend to decrease the truth value of `a` being friend with `b`.

These are different scenarios and ways in which the framework pushes parametric groundings to verify logical constraints. One can easily imagine how the LTN loss can be used as an additional loss term when training neural networks or embeddings to find a balanced optimum that also satisfies a knowledgebase.

A.2 Product Real Logic and Prenex Normal Form

The study conducted by van Krieken *et al.* (2022) evaluated a range of operators for differentiability and found Product Real Logic to be the current state-of-the-art operator semantics for differentiable fuzzy logics. This set of semantics uses the product t-norm $T_P(x, y) = xy$, its dual t-conorm $S_P(x, y) = x + y - xy$, the standard negation $N_S(x) = 1 - x$, and the material implication. The universal quantifier uses the log-product aggregator $(\log \circ A_{T_P})(x_1, \dots, x_n) = \sum_{i=1}^n \log(x_i)$, and the existential quantifier uses a smooth maximum.

A limitation of this set of semantics is that it combines operators in both the standard space and the logarithm space, making it challenging to handle certain formulas. For example, a formula such as $(\forall u P(u)) \vee (\forall v Q(v))$ cannot be grounded as is, as the \forall operator outputs a log truth degree while the \vee operator expects a normal truth degree. One potential solution is to transform the formula into Prenex Normal Form (PNF) $\forall u \forall v (P(u) \vee Q(v))$, but this adds considerable complexity as we now need to ground combinations of individuals from `u` and `v`. PNF formulas that contain universal quantifiers within the scope of existential quantifiers, such as $\forall u \exists v \forall w P(u, v, w)$, are even more difficult to handle. logLTN, on the other hand, is simpler to work with in these cases.

³ ϕ is semantically equivalent to $f(a, b) \rightarrow f(b, a)$ if we use a material implication defined as $p \rightarrow q \equiv \neg p \vee q$.

A.3 Simplification of Log Sigmoid and Log Softmax

Given the sigmoid function $S(x) = \frac{1}{1+e^{-x}}$, for large negative values of x , we have $\log(S(x)) = \log\left(\frac{1}{1+N}\right) = \log(1) - \log(1+N) \approx -N$ where N is a large number. The derivative is also simple. Given that $\frac{\partial S(x)}{\partial x} = S(x)(1 - S(x))$, we have:

$$\frac{\partial \log(S(x))}{\partial x} = 1 - S(x) \quad (30)$$

Similarly, given that the softmax function $\sigma(\mathbf{z})_i = \frac{e^{z_i}}{\sum_{j=1}^K e^{z_j}}$ over a vector \mathbf{z} of K values, $i = 1, \dots, K$, has the derivatives $\frac{\partial \sigma(\mathbf{z})_i}{\partial z_j} = \sigma(\mathbf{z})_i(\delta_{ij} - \sigma(\mathbf{z})_j)$, we have:

$$\frac{\partial \log(\sigma(\mathbf{z})_i)}{\partial z_j} = \delta_{ij} - \sigma(\mathbf{z})_j \quad (31)$$

$$\text{where } \delta_{ij} = \begin{cases} 1 & i = j \\ 0 & i \neq j \end{cases} .$$

B Experiments

B.1 Semantic PASCAL-Part Dataset

The semantic PASCAL-Part dataset is a simplified version of the PASCAL-Part dataset introduced by Chen *et al.* (2014). The goal is to train a type classifier $\text{is}(x, \text{bottle})$, $\text{is}(x, \text{cap})$, etc., that predicts the type of an object within a bounding box x , and to train a relation predictor $\text{partOf}(x, y)$ that determines if one bounding box x is part of another bounding box y .

B.1.1 Constraints

Training is guided by three constraints based on ground truth examples, one for labeled type examples, one for pairs of positive examples for partOf , and one for pairs of negative examples. Note that the negative pairs are always sampled in bounding boxes belonging to the same image.

$$\forall \text{diag}(x_{\text{label}}, \text{label}) \text{ is}(x_{\text{label}}, \text{label}) \quad (32)$$

$$\forall \text{pairs}_+ \text{ partOf}(\text{pairs}_+[0], \text{pairs}_+[1]) \quad (33)$$

$$\forall \text{pairs}_- \neg \text{partOf}(\text{pairs}_-[0], \text{pairs}_-[1]) \quad (34)$$

$$(35)$$

Where $\text{diag}(x_{\text{label}}, \text{label})$ is a special quantification that aggregates only arranged pairs of bounding boxes and their labels, pairs_+ is a batch of positive examples of partOf , pairs_- is a batch of negative examples of partOf .

There are two constraints stating that partOf is antisymmetric and antireflexive.

$$\forall \text{pairs} \neg (\text{partOf}(\text{pairs}[0], \text{pairs}[1]) \wedge \text{partOf}(\text{pairs}[1], \text{pairs}[0])) \quad (36)$$

$$\forall x \neg \text{partOf}(x, x) \quad (37)$$

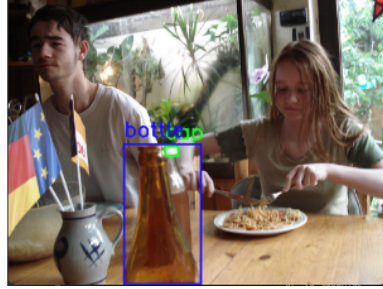
Finally, and most importantly, there are mereological constraints that the types and their meanings. The mereological constraints are based on the ontologies in Table 4 rearranged in the shape of (38) and (39).

$$\forall x, y \text{ is}(x, \text{bottle}) \wedge \text{partOf}(y, x) \rightarrow (\text{is}(y, \text{cap}) \vee \text{is}(x, \text{body})) \quad (38)$$

$$\forall x, y \text{ is}(x, \text{cap}) \wedge \text{partOf}(x, y) \rightarrow \text{is}(y, \text{bottle}) \quad (39)$$

B.1.2 Features

This setup has been previously implemented by Donadello *et al.* (2017); van Krieken *et al.* (2019). In these previous works, the bounding boxes were grounded with the object class predictions produced by an object detector trained on the PASCAL-Part dataset. This means that LTN was only used



(a) Nonviolation (a cap port of a bottle)



(b) Violation (a plant part of another plant)

Figure 3: Examples of false positives on Semantic PASCAL-Part. Green is predicted in blue.

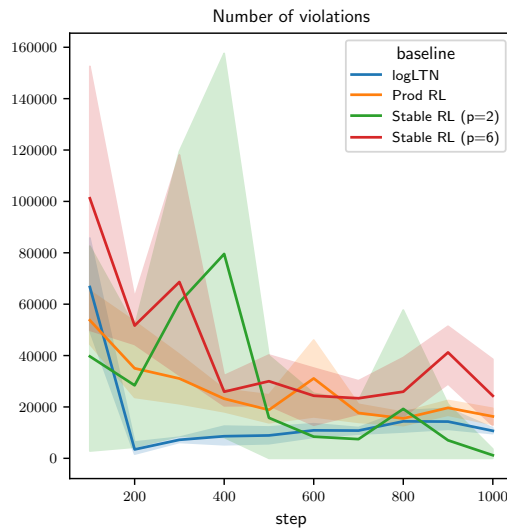


Figure 4: Violations over training time. The first 100 training steps are used for pretraining without the mereological constraints.

to correct the predictions of the detector. In contrast, we increased the difficulty by grounding the bounding boxes with a latent vector of 1024 features, which is produced by an intermediate layer of the FasterRCNN Ren *et al.* (2017). This means that LTN must also learn the final layers of the object classifier. In addition, we included the coordinates of each bounding box and their overlapping ratio when grounding the pairs.

For a work that trains an object detector architecture end-to-end on all types using LTN, refer to Manigrasso *et al.* (2021).

B.1.3 Violation metrics

In addition to the standard accuracy metrics for each predictor (PR AUC for the part-of predictor and balanced accuracy for the type predictor), we also assess their combined performance by measuring *violations* of the mereological constraints. It's important to note that not all misclassifications are equal. For instance, if a model predicts a cap inside a plant, it suggests that the system has learned less from prior knowledge compared to a model that misclassifies the cap in a different context, such as a wrong bottle.

This concept is visually represented in Figure 3. Our results demonstrate that not only does logLTN exhibit significantly fewer violations, but it also reaches this outcome much faster compared to other baseline approaches, as shown in Figure 4.

Whole	Parts
aeroplane	artifact_wing, body, engine, stern, wheel
bicycle	chain_wheel, handlebar, headlight, saddle, wheel
bird	animal_wing, beak, tail, eye, head, leg, neck, torso
bottle	body, cap
bus	bodywork, door, headlight, license_plate, mirror, wheel, window
car	bodywork, door, headlight, license_plate, mirror, wheel, window
cat	ear, tail, eye, head, leg, neck, torso
cow	ear, horn, muzzle, tail, eye, head, leg, neck, torso
dog	ear, muzzle, nose, tail, eye, head, leg, neck, torso
horse	ear, hoof, muzzle, tail, eye, head, leg, neck, torso
motorbike	handlebar, headlight, saddle, wheel
person	arm, ear, eyebrow, foot, hair, hand, mouth, nose, eye, head, leg, neck, torso
pottedplant	plant, pot
sheep	ear, horn, muzzle, tail, eye, head, leg, neck, torso
train	coach, headlight, locomotive
tvmonitor	screen
boat	
chair	
sofa	
diningtable	

Table 4: Full ontologies in Semantic PASCAL-Part

Baseline	Operator	Parameter	Schedule
logLTN	\exists : LME	α	Linear: [1, 4]
Prod RL	\exists : pM	p	Linear: [1, 6]
Stable RL	\exists : pM	p	Linear: [1, 6]

Linear $[a, b]$: the parameter increases linearly from a to b over the training steps,

$$\text{pM}(x_1, \dots, x_n | p) = \left(\frac{1}{n} \sum_{i=1}^n x_i^p\right)^{\frac{1}{p}},$$

$$\text{pME}(x_1, \dots, x_n | p) = 1 - \left(\frac{1}{n} \sum_{i=1}^n (1 - x_i)^p\right)^{\frac{1}{p}}.$$

Table 5: Overview of the hyperparameters used in the experiments for each fuzzy operator configuration.

B.2 Implementation Details

logLTN is made available as a subpackage of the LTN library.⁴ Table 6 details the neural models used in each experimental task and Table 5 details the hyperparameters of the baselines. The Adam optimizer is trained with a learning rate of 0.002 in the clustering task and a learning rate of 0.001 for the MNISTAdd and Semantic Image Interpretation (SII) task. We run our experiments on a machine equipped with a Tesla T4 GPU.

C Theory

C.1 Log-Negations

C.1.1 Proof of Theorem 1

Theorem 1. *The log-negation of a sigmoid function $S(x) = \frac{1}{1+e^{-x}}$, $x \in \mathbb{R}$, simplifies as*

$$(\log \circ \text{N}_S)(S(x)) = \log(S(x)) - x \tag{6}$$

⁴<https://github.com/logictensornetworks/logictensornetworks>

Proof.

$$\begin{aligned}
(\log \circ N_S)(x) &= \log(1 - S(x)) = \log(S(x)) + \log\left(\frac{1 - S(x)}{S(x)}\right) \\
&= \log(S(x)) + \log\left(\frac{1 - \frac{e^x}{e^x + 1}}{\frac{e^x}{e^x + 1}}\right) \\
&= \log(S(x)) + \log\left(\frac{e^x + 1 - e^x}{e^x}\right) \\
&= \log(S(x)) - x \quad \square
\end{aligned}$$

C.1.2 Proof of Theorem 2

Theorem 2. *The log-negation of a softmax function $\sigma(\mathbf{z})_i = \frac{e^{z_i}}{\sum_{j=1}^K e^{z_j}}$, where $\mathbf{z} = (z_1, \dots, z_K) \in \mathbb{R}^K$ is a vector of K real values, and $i = 1, \dots, K$, simplifies as*

$$(\log \circ N_S)(\sigma(\mathbf{z})_i) = \log(\sigma(\mathbf{z})_i) + \log\left(\sum_{\substack{j=1 \\ j \neq i}}^K e^{z_j}\right) - z_i \quad (7)$$

Proof.

$$\begin{aligned}
(\log \circ N_S)(\sigma(\mathbf{z})_i) &= \log(1 - \sigma(\mathbf{z})_i) \\
&= \log(\sigma(\mathbf{z})_i) + \log\left(\frac{1 - \sigma(\mathbf{z})_i}{\sigma(\mathbf{z})_i}\right) \\
&= \log(\sigma(\mathbf{z})_i) + \log\left(\frac{1 - \frac{e^{z_i}}{\sum_{j=1}^K e^{z_j}}}{\frac{e^{z_i}}{\sum_{j=1}^K e^{z_j}}}\right) \\
&= \log(\sigma(\mathbf{z})_i) + \log\left(\frac{\sum_{j=1}^K e^{z_j} - e^{z_i}}{e^{z_i}}\right) \\
&= \log(\sigma(\mathbf{z})_i) + \log\left(\sum_{\substack{j=1 \\ j \neq i}}^K e^{z_j}\right) - z_i \quad \square
\end{aligned}$$

Task	Predicate	Model	Output layer
Clustering	$C(x, c)$	Dense(16)*, Dense(16)*, Dense(16)	Softmax
MNISTAdd	$\text{is_digit}(x, d)$	Conv(6, 5)*, MP(2, 2), Conv(16, 5)*, MP(2, 2), Dense(100)*, Dense(84)*, Dense(10)	Softmax
SII	$\text{type}(x, t)$	Dense(512)*, Dense(256)*, Dense(256)*, Dense(128)*, Dense(128)	Softmax
SII	$\text{partof}(x, y)$	Concat($\text{type}_{\text{Model}}(x), \text{type}_{\text{Model}}(y)$), Dense(512)*, Dense(256)*, Dense(256)*, Dense(128)*, Dense(128)	Sigmoid

*: layer ends with an elu activation,
Dense(k): linear layer with k units,
Conv(f, k): 2D convolution layer with f filters and a kernel of size k ,
MP(w, h): max pooling operation with a $w \times h$ pooling window.

Table 6: Overview of the neural architectures used in each task.

C.2 Relaxation of the Disjunction

C.2.1 Bounds of LogSumExp

We start from Equation (10) and subtract $-\frac{\log(n)}{a}$ in all parts of the inequality:

$$\max(\mathbf{x}) - \frac{\log(n)}{\alpha} \leq \text{LSE}(\mathbf{x} \mid \alpha, C) - \frac{\log(n)}{\alpha} \leq \max(\mathbf{x}) \quad (40)$$

And:

$$\text{LSE}(\mathbf{x} \mid \alpha, C) - \frac{\log(n)}{\alpha} = \frac{1}{\alpha} \left(C + \log \left(\sum_{i=1}^n e^{\alpha x_i - C} \right) - \log(n) \right) \quad (41)$$

$$= \frac{1}{\alpha} \left(C + \log \left(\frac{\sum_{i=1}^n e^{\alpha x_i - C}}{n} \right) \right) \quad (42)$$

$$= \text{LME}(\mathbf{x} \mid \alpha, C) \quad (43)$$

Given (40) and (43), we obtain the inequality for LME:

$$\max(\mathbf{x}) - \frac{\log(n)}{\alpha} \leq \text{LME}(\mathbf{x} \mid \alpha, C) \leq \max(\mathbf{x}) \quad (44)$$

C.3 De Morgan's Inequalities

C.3.1 Proof of Theorem 3

Theorem 3. *Let P and Q be two formulas. We can show that*

$$\mathcal{G}(\neg(P \wedge Q)) \geq \mathcal{G}(\neg P \vee \neg Q) \quad (16)$$

$$\mathcal{G}(\neg(P \vee Q)) \geq \mathcal{G}(\neg P \wedge \neg Q) \quad (17)$$

$$\mathcal{G}(\neg(\forall u P(u))) \geq \mathcal{G}(\exists u \neg P(u)) \quad (18)$$

$$\mathcal{G}(\neg(\exists u P(u))) \geq \mathcal{G}(\forall u \neg P(u)) \quad (19)$$

Proof. Let $\mathcal{G}(P) = x$, $\mathcal{G}(Q) = y$, and $\mathcal{G}(P(u)) = [x_1, \dots, x_n]$, where $x, y, x_1, \dots, x_n \in [0, 1]$. Grounding the operators with the definitions of Section 3.1, we need to prove:

$$\text{N}_S(\text{T}_P(x, y)) \geq \text{S}_M(\text{N}_S(x), \text{N}_S(y)) \quad (45)$$

$$\text{N}_S(\text{S}_M(x, y)) \geq \text{T}_P(\text{N}_S(x), \text{N}_S(y)) \quad (46)$$

$$\text{N}_S(\text{A}_{\text{T}_P}(x_1, \dots, x_n)) \geq \text{A}_{\text{S}_M}(\text{N}_S(x_1), \dots, \text{N}_S(x_n)) \quad (47)$$

$$\text{N}_S(\text{A}_{\text{S}_M}(x_1, \dots, x_n)) \geq \text{A}_{\text{T}_P}(\text{N}_S(x_1), \dots, \text{N}_S(x_n)) \quad (48)$$

(45) and (46) are specializations of the other two equations by working with $n = 2$ values. We focus on proving (47). Indeed, we can easily retrieve (48) from (47).

Equivalence of (47) and (48) Posing $x'_i = 1 - x_i$ for $i = 1 \dots n$, we have:

$$\text{N}_S(\text{A}_{\text{T}_P}(x_1, \dots, x_n)) \geq \text{A}_{\text{S}_M}(\text{N}_S(x_1), \dots, \text{N}_S(x_n)) \quad (49)$$

$$\iff \text{N}_S(\text{N}_S(\text{A}_{\text{T}_P}(x_1, \dots, x_n))) \leq \text{N}_S(\text{A}_{\text{S}_M}(\text{N}_S(x_1), \dots, \text{N}_S(x_n))) \quad (50)$$

$$\iff \text{A}_{\text{T}_P}(x_1, \dots, x_n) \leq \text{N}_S(\text{A}_{\text{S}_M}(\text{N}_S(x_1), \dots, \text{N}_S(x_n))) \quad (51)$$

$$\iff \text{A}_{\text{T}_P}(\text{N}_S(x'_1), \dots, \text{N}_S(x'_n)) \leq \text{N}_S(\text{A}_{\text{S}_M}(x'_1, \dots, x'_n)) \quad (52)$$

$$\iff \text{N}_S(\text{A}_{\text{S}_M}(x'_1, \dots, x'_n)) \geq \text{A}_{\text{T}_P}(\text{N}_S(x'_1), \dots, \text{N}_S(x'_n)) \quad (53)$$

Proof of (47) In the left-hand side of the inequality, we have:

$$\text{N}_S(\text{A}_{\text{T}_P}(x_1, \dots, x_n)) = 1 - \prod_{i=1}^n x_i \quad (54)$$

and in the right-hand side:

$$A_{S_M}(N_S(x_1), \dots, N_S(x_n)) = \max_{i=1}^n (1 - x_i) = 1 - \min_{i=1}^n (x_i) \quad (55)$$

Replacing them in the original inequality, and denoting $j = \operatorname{argmin}_{i=1}^n (x_i)$, we obtain:

$$1 - \prod_{i=1}^n x_i \geq 1 - \min_{i=1}^n (x_i) \quad (56)$$

$$\iff \prod_{i=1}^n x_i \leq \min_{i=1}^n (x_i) \quad (57)$$

$$\iff x_j \prod_{\substack{i=1 \\ i \neq j}}^n x_i \leq x_j \quad (58)$$

$$\iff \prod_{\substack{i=1 \\ i \neq j}}^n x_i \leq 1 \quad (59)$$

Which is true because all $x_i \in [0, 1]$. □

C.3.2 Tightness of the bounds

We provide an analysis of the tightness of the bounds of the De Morgan's inequalities. We measure the tightness for the quantifier variants of the inequalities, as this generalizes to the case $n = 2$.

Tightness of (47) Let us first characterize the maximum value of the bound. We are interesting in finding the values (x_1^*, \dots, x_n^*) that maximize the difference of the two members in (47).

$$(x_1^*, \dots, x_n^*) = \operatorname{argmax}_{(x_1, \dots, x_n)} \Delta_{\wedge}(x_1, \dots, x_n) \quad (60)$$

with

$$\Delta_{\wedge}(x_1, \dots, x_n) = N_S(A_{T_P}(x_1, \dots, x_n)) - A_{S_M}(N_S(x_1), \dots, N_S(x_n)) \quad (61)$$

$$= (1 - \prod_{i=1}^n x_i) - (1 - \min_{i=1}^n (x_i)) = \min_{i=1}^n (x_i) - \prod_{i=1}^n x_i \quad (62)$$

Let $j = \operatorname{argmin}_{i=1}^n (x_i)$.

$$\Delta_{\wedge}(x_1, \dots, x_n) = x_j - \prod_{\substack{i=1 \\ i \neq j}}^n x_i = x_j (1 - \prod_{\substack{i=1 \\ i \neq j}}^n x_i) \quad (63)$$

For any set of values, we have $\Delta_{\wedge}(x_j, \dots, x_j) \geq \Delta_{\wedge}(x_1, \dots, x_n)$, as $(1 - x_j^{n-1}) \geq (1 - \prod_{\substack{i=1 \\ i \neq j}}^n x_i)$ given that $x_j = \min_{i=1}^n (x_i)$. Therefore, (x_1^*, \dots, x_n^*) is actually a tuple of the same value taken n times, and we reduce the search to:

$$x^* = \operatorname{argmax}_x \Delta_{\wedge}(x) = \operatorname{argmax}_x x - x^n \quad (64)$$

Given that $x \in [0, 1]$, we find by first and second order derivative analysis that $\Delta_{\wedge}(x)$ is concave on the whole domain and has a single maximum at:

$$x^* = n^{-\frac{1}{n-1}} \quad (65)$$

For $n = 2$, that is, when applying the De Morgan's law to a simple conjunction of two terms x_1 and x_2 , the bound of the inequality is maximal when $x_1 = x_2 = 0.5$, giving $\Delta_{\wedge} = 0.25$. However, on average, the bound is smaller. By sampling $10e4 \times 10e4$ points linearly on the domain $[0, 1] \times [0, 1]$, we find an average $\Delta_{\wedge} = 0.083167$. We visualize the bound of the inequality in Figure 5. It is zero when any $x_i = 0$ or $x_i = 1$, in which case the De Morgan's laws are verified.

For larger n , that is, when applying the quantifier equivalent of the De Morgan's law, the maximal value of the bound becomes larger. For example, with $n = 8$, the bound is maximal for $x_1 = \dots = x_8 \approx 0.743$, with $\Delta_{\wedge} \approx 0.650$. However, on average, the bound stays small. By sampling $10e8$ points linearly in the domain $[0, 1]^8$, we have an average bound of 0.07135.

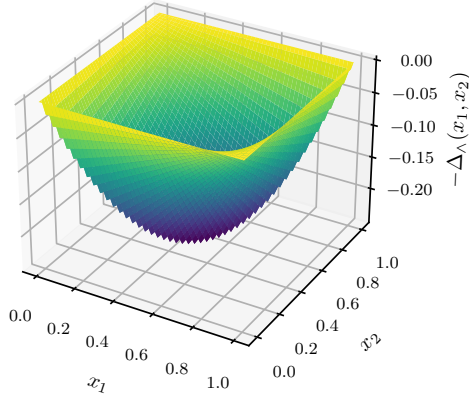


Figure 5: De Morgan's inequality bound $-\Delta_{\wedge}(x_1, x_2)$

Tightness of (48) As we have shown in Section C.3.1, (48) is equivalent to (47) by replacing the input values with $x'_i = 1 - x_i$ for $i = 1 \dots n$. Therefore, the maximum value of the bound is the same, except that it happens on a complement set of value. We have:

$$x^* = \operatorname{argmax}_x \Delta_{\vee}(x) \quad (66)$$

$$= \operatorname{argmax}_x N_S(A_{S_M}(x, \dots, x)) - A_{T_P}(N_S(x), \dots, N_S(x)) \quad (67)$$

$$= \operatorname{argmax}_x 1 - x - (1 - x)^n \quad (68)$$

$$= 1 - n^{-\left(\frac{1}{n-1}\right)} \quad (69)$$

For $n = 2$, when applying the De Morgan's law to a simple disjunction of two terms x_1 and x_2 , Δ_{\vee} is maximal when $x_1 = x_2 = 0.5$. We find again that the peak is $\Delta_{\vee} = 0.25$, and by sampling $10e4 \times 10e4$ points linearly on the domain $[0, 1] \times [0, 1]$, we find an average $\Delta_{\vee} = 0.083167$.

For $n = 8$, this time the bound is maximal when $x_1 = \dots = x_8 \approx 0.257$, with $\Delta_{\vee} \approx 0.650$. Sampling $10e8$ points linearly in $[0, 1]^8$, we still get an average bound of 0.07135.

C.4 Common Fuzzy Properties for logLTN

We provide an overview of common fuzzy properties that are verified by the operator configuration in Table 7. The distributivity of \wedge over \vee for logLTN is the only new property and can be demonstrated easily. Let $\mathcal{G}(P) = x$, $\mathcal{G}(Q) = y$, and $\mathcal{G}(R) = z$ be the grounding of three predicates. We have:

$$\mathcal{G}(P \wedge (Q \vee R)) = \mathcal{G}((P \wedge Q) \vee (P \wedge R)) \quad (70)$$

$$\iff x \max(y, z) = \max(xy, xz) \quad (71)$$

Property	logLTN	Prod RL	Stable RL
Commutativity of \wedge, \vee	✓	✓	✓
Associativity of \wedge, \vee	✓	✓	✓
De Morgan's laws for \wedge and \vee		✓	✓
Material Implication	✓	✓	✓
Distributivity of \wedge over \vee	✓		
Distributivity of \vee over \wedge			
Double negation, i.e. $\mathcal{G}(\neg\neg p) = \mathcal{G}(p)$	✓	✓	✓
Law of non-excluded middle, i.e. $\mathcal{G}(p \wedge \neg p) = 0$			
Law of non-contradiction, i.e. $\mathcal{G}(p \vee \neg p) = 1$			
Conjunction elimination, i.e. $\mathcal{G}(p \wedge p) \leq \mathcal{G}(p)$	✓	✓	✓
Disjunction amplification, i.e. $\mathcal{G}(p \vee p) \geq \mathcal{G}(p)$	✓	✓	✓
\forall defined as a generalization of \wedge	✓	✓	
\exists defined as a generalization of \vee	✓		
De Morgan's laws for \forall and \exists			

Table 7: Fuzzy properties for logLTN, Product Real Logic (Prod RL), and Stable Product Real Logic (Stable RL).